Spin-dependent scattering of deeply bound nucleons

C. A. Miller,[1] K. H. Hicks,[1,4] R. Abegg,[1,‖] M. Ahmad,[2,*] N. S. Chant,[3] D. Frekers,[1,†] P. W. Green,[1] L. G. Greeniaus,[2] D. A. Hutcheon,[1] P. Kitching,[2] D. J. Mack,[2,‡] W. J. McDonald,[2] W. C. Olsen,[2] R. Schubank,[5] P. G. Roos,[3] and Y. Ye[2,§]

[1]*TRIUMF, 4004 Wesbrook Mall, Vancouver, British Columbia, Canada V6T 2A3*

[2]*University of Alberta, Edmonton, Alberta, Canada T6G 2N5*

[3]*University of Maryland, College Park, Maryland 20742*

[4]*Ohio University, Athens, Ohio 45701*

[5]*University of Saskatchewan, Saskatoon, Saskatchewan, Canada*

(Received 7 August 1996; revised manuscript received 5 December 1997)

Exclusive measurements of the analyzing power and two spin-transfer observables for nucleon knockout from an ^{16}O target are presented, at kinematic conditions chosen to emphasize interactions in the nuclear interior. The analyzing power data are substantially reduced in comparison with values calculated in the distorted wave impulse approximation (DWIA) using the free nucleon-nucleon interaction, particularly for knockout of the deeply bound $1s_{1/2}$ nucleons. Inclusion of density dependence for the interaction in the calculations improves the agreement with the data, but does not provide a satisfactory description for nucleon knockout from ^{16}O. Spin-orbit distortions are shown to strongly affect the DWIA predictions of the $1s_{1/2}$ analyzing powers over most of the experimental kinematic range, but notably not near the points of negligible recoil momentum. Hence these data offer constraints on the optical potentials and independently on the two-body effective interaction. [S0556-2813(98)02104-9]

PACS number(s): 25.40.Ep, 24.70.+s, 24.10.Eq, 13.75.−n

I. INTRODUCTION

Exclusive measurements of nucleon knockout tell us about both the bound state of the struck nucleon and the nature of the strong interaction in nuclear matter. When the focus is on the latter, kinematic selection of deeply bound nucleons offers the opportunity to emphasize the nuclear interior where the matter density is higher and more uniform. Many contemporary models predict a modification of the interaction between the bound nucleon and the projectile deep inside the nuclear medium. For instance, some models predict a small change in the radius of the nucleon [1] to explain anomalously large cross sections for deeply penetrating probes like the K^+, whereas other models invoke a density-dependent effective mass for the nucleon in the nuclear interior, based on either relativistic [2] or nonrelativistic [3,4] dynamics.

Experimental evidence for medium modifications of the nucleon-nucleon (NN) interaction has been available for over a decade. The paper by Hintz *et al.* [5] presents the energy dependence of cross sections for excitation of high-spin natural parity states by proton inelastic scattering. They show that at lower proton energies, where the density dependence of the NN interaction is expected to be stronger, the disagreement between theory and experiment increases. This result, along with other measurements described below, suggested that the nuclear medium effects on the NN interaction could be substantial and has inspired much theoretical work. Obvious mechanisms such as Pauli blocking were shown to have only a small effect on the calculations, and so there arose new interest in identifying other possible mechanisms.

Further evidence for medium modification of the NN interaction was seen in inclusive polarized-proton scattering data [6–9]. Such measurements include scattering from single neutrons and protons averaged over all bound states, a process known as inclusive quasielastic scattering. Carey *et al.* [6] measured polarization transfer observables for quasielastic scattering from ^{208}Pb and ^{2}H at 500 MeV. Although not published at that time, the analyzing power and polarization data from this experiment appeared later in a theoretical paper that compared the data and calculations. These data show a large ($\sim$40%) suppression of both the analyzing power and the final state polarization, in comparison with free NN scattering [2]. Calculations based on the Dirac equation with large attractive scalar and repulsive vector potentials, which enhance the lower components of the Dirac spinors in the nuclear medium, are in good agreement with the inclusive quasielastic data [2,10]. On the other hand, calculations based on the Schrödinger equation [11] fail to replicate the analyzing power suppression seen in the quasielastic data, and instead predict values of the final-state polarization nearly the same as for free NN scattering. Polarization transfer observables also show medium modifications to a lesser extent [8–10].

More recent studies of proton-nucleus scattering in a relativistic approach [12] have resulted in effective interactions similar to, but more complete than, those based on the m^* approximation in Ref. [2]. The medium effects in these effective interactions derived from the IA2 set of Lorentz invariant amplitudes again arise from distortions of plane wave Dirac spinors in the nuclear medium. The observable effect

*Present address: Albert Einstein College of Medicine, Bronx, NY 10461.

†Present address: University of Münster, Münster, Germany.

‡Present address: CEBAF, 12000 Jefferson Ave., Newport News, VA 23606.

§Present address: Peking University, Beijing, China.

‖Deceased.

is nearly equivalent to adding a short-ranged repulsive contribution to the real central part of the proton-nucleus interaction [13] of nonrelativistic models. One set of these effective interactions is designed for application to inelastic scattering [14], and might also be suitable for use in future $(p,2p)$ calculations.

Brown *et al.* have proposed a new approach to medium modifications that is based on considerations of a partial restoration of chiral symmetry in nuclei [15]. This results in a lowering of the effective mass of the ρ meson which dominates the short-range repulsive part of the *NN* interaction. Recent polarization transfer data from the Indiana University Cyclotron Facility (IUCF) show that the spin-longitudinal cross section for inelastic scattering to the 6^- stretched state in ^{28}Si is overpredicted by a factor of two in calculations using the free *NN* interaction [16]. A modified *t* matrix which includes a reduced in-medium ρ meson mass can reproduce the data [16]. Similar evidence for this effect is found in data for stretched states in ^{208}Pb at 318 MeV [17]. While the issues surrounding the effective ρ-meson mass are far from settled, the data clearly indicate that a medium modification to the proton-nucleus interaction is needed.

In contrast to these efforts to identify specific theoretical mechanisms, Kelly and co-workers have used nonrelativistic effective interactions, containing semiempirical parameterizations for density dependence, to investigate the *NN* interaction in nuclear matter. The parameters in this model are constrained by simultaneous fits to experimental elastic and inelastic scattering data. This class of models [18] is based on the premise of the local density approximation, with all the ingredients of Pauli blocking included. A comparison of the success of Kelly's effective interaction with that of a relativistic model [19] suggests that the former model gives a better representation of the density dependence at energies between 200–400 MeV, whereas the relativistic model is in better agreement with the data near 500 MeV. The apparent success of different approaches to modifications of the *NN* interaction in the nuclear medium suggests the need for more data that are sensitive to interactions occurring in the highest density region at the center of the nucleus where the effects will be strongest.

In such an investigation, exclusive measurements have some significant advantages. First, the *p*-*p* and *n*-*p* interactions can be studied separately instead of being averaged together. Also, the half-off-shell kinematic conditions of each scattering event are determined experimentally instead of being averaged, resulting in more explicit information. Most importantly, because the residual nucleus energy is determined experimentally, knockout from individual nuclear orbitals can be distinguished. To maximize medium effects, we may therefore select events corresponding to knockout from an orbital whose wave function has the bulk of its strength within the nuclear volume. The $1s_{1/2}$ orbital in nuclei with $A>12$ satisfies this criterion and further simplifies the interpretation of the data by precluding any effective initial polarization of the struck nucleon due to distortion effects [20]. Kinematically emphasizing the nuclear interior reduces uncertainties associated with reactions which may be more sensitive to the nuclear surface. For example, the local density approximation is most suspect near the nuclear surface where the density gradient is large. Some exclusive measurements of $1s_{1/2}$ knockout have been reported by both the present authors [10,21] and by others [22]. Evidence was found to support our expectations of enhanced sensitivity to medium effects in such experiments. Here we report further data for spin transfer coefficients, and present comprehensive comparisons of all our data with recently refined theoretical calculations for this reaction, using several different models for the main interaction.

In the present work, the momenta of both the scattered and ejected protons were measured in coincidence in order to determine the binding energy of the struck nucleon. The choice of a $1p$ shell nucleus, ^{16}O, as well as the highest-possible beam energy of 504 MeV were defined by the need to minimize the effects of absorption on the final state nucleons. By comparing knockout of $1s$ and $1p$ nucleons, we can sample the medium modifications at different nuclear densities, and compare the results with the predictions of the relativistic model, as well as various nonrelativistic density-dependent calculations. The measurements were done at several angle pairs to vary the scattering kinematics and better test the models. We present the data for each angle pair as a function of the energy of the most energetic final state proton. This type of presentation is illuminating for our purposes because the dependence of the two-body nucleon-nucleon kinematics on the energy sharing in the 3-body final state is such that the free *N*-*N* analyzing power is only weakly dependent on this variable. (This will be later illustrated in Fig. 9). Hence any strong variation of the $(p,2p)$ analyzing power with energy sharing can be associated with spin-orbit distortions in the case of *s* state knockout, and also struck nucleon polarization in the case of *p* state knockout.

We present here both analyzing powers and the first spin-transfer observables measured for the $(p,2p)$ reaction at intermediate energies. The details of the experiment are given in the next section. Because of the nature of the target, cross sections were not extracted. However, cross sections measured under similar kinematic conditions have been reported [23], and will be compared with theoretical predictions in this paper.

II. EXPERIMENTAL DETAILS

The experiment was carried out in the proton hall at TRIUMF with an incident polarized proton beam of energy 504 MeV. Both normal $(\hat{n})$ and sideways $(\hat{s})$ beam polarizations were used, with typical beam currents averaging 20 nA. The spins were flipped on a cycle time of about 2.5 minutes, with typical beam polarization of 70% for either $\hat{n}$ or $\hat{s}$ directions. The small components of the polarization in other directions were less than 3%. The polarization was monitored continuously with an in-beam polarimeter (IBP) [24] based on *p*-*p* scattering from a polyethylene target at $\theta_{\rm lab}=17°$. After subtracting accidental coincidences and correcting for the carbon background, the beam polarization was measured to an accuracy of typically 0.01. The IBP also served as a beam current monitor.

The ^{16}O target was in the form of a waterfall in a small chamber at a pressure of 0.33 atmosphere contained by thin mylar vacuum windows. This small chamber was mounted inside the vacuum chamber that is coupled to the medium resolution spectrometer (MRS). The target thickness was ap-

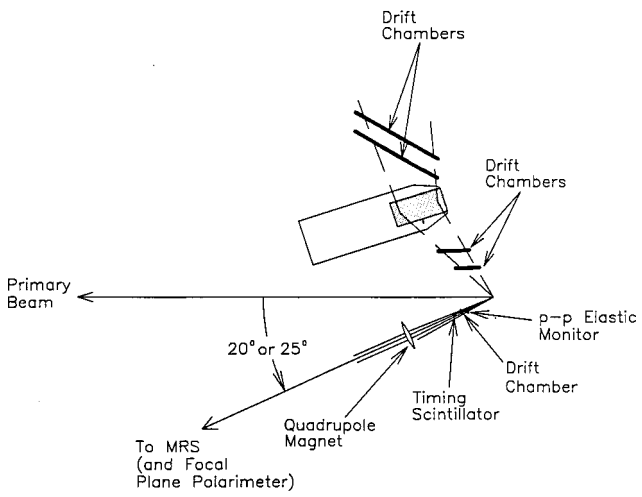

FIG. 1. Experimental setup for the $^{16}O(p,2p)$ experiment. The high-energy proton was detected in the medium resolution spectrometer (MRS) which is only partially shown, and the low-energy proton was detected by the nonfocusing magnetic spectrometer on the other side of the beamline.

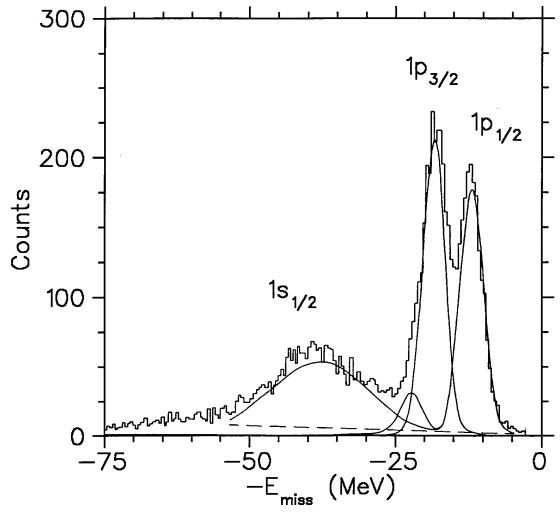

FIG. 2. Missing mass spectrum for the $^{16}O(p,2p)$ reaction at 504 MeV. The two sharp peaks are from p-shell knockout, and the broad peak is from s-shell knockout.

proximately 150 mg/cm^2, regulated by the flow of water through the pump, and monitored by p-p elastic events triggered by a plastic scintillator in coincidence with one of the magnetic spectrometers. The MRS is a QD system, and was used to detect the high-energy proton in the $(p,2p)$ coincidence. It has an effective solid angle of about 3 msr and a scattering-angle acceptance of about 3°. The waterfall target and the MRS have been described in Refs. [25] and [26], respectively.

On the other side of the beamline was a nonfocusing magnetic spectrometer consisting of a dipole magnet between two sets of vertical-drift chambers (VDCs). This configuration is shown in Fig. 1. The set of two VDCs between the target and magnet contained both X and U wire planes for measuring both X, the bend-plane coordinate, and the U coordinate tilted at 30° to X. Y was deduced from a linear combination of X and U. The set of two VDCs after the magnet contained only X planes. The acceptance covered an angular range of 6°. Proton elastic scattering was used to derive a momentum calibration. The spectrometer could be moved a limited distance on linear rails to make this possible. The energy resolution of the system was dominated by tracking resolution and multiple scattering. The magnet gap was filled with helium gas to reduce the latter. Figure 2 shows a typical spectrum of reconstructed missing mass. An energy resolution of about 4.5 MeV (FWHM) was obtained, which allowed extraction of yields for the $1p_{1/2}$ and $1p_{3/2}$ knockout using peak-fitting procedures. The $1s_{1/2}$ knockout is the broad peak at larger missing mass values.

The computer dead-time was monitored continuously using a pulser signal at a randomized rate proportional to the beam current. The wire chamber efficiencies were determined by counting the events that were recorded in 3 of the 4 wire planes for otherwise good tracks, and comparing this with the number of events where all four planes were hit. Typical values for the wire chamber efficiencies were 0.95 per plane. The maximum useful beam current was defined by the need to limit the fraction of events lost due to multiple tracks in the VDCs. Corrections were applied for the associated tracking inefficiencies.

Following the tracking drift chambers near the MRS focal plane was a focal plane polarimeter (FPP). The FPP measured the polarization of the high-energy proton by secondary scattering from a 13.5 cm thick carbon slab. Position information from 3 pairs of X-Y delay-line wire chambers after the scattering vertex in the carbon slab was used to determine the polar and azimuthal scattering angles. Fits to the cross section and analyzing power between polar angles of 5° and 20° for scattering from carbon were used to determine the polarization. Details of this technique are described in Ref. [27].

The kinematics for the measurements were chosen with a view to keeping the recoil momentum of the residual nucleus small for knockout of 1s-shell protons. Care was also taken to avoid excessively asymmetric kinematics resulting in one small final state proton energy, which might cast doubt on the validity of the reaction model. However, angles were chosen as asymmetrical as was considered safe, to maximize the polarization asymmetries and to maximize their predicted sensitivity to medium effects according to preliminary DWIA calculations. The angles in the laboratory frame included either 20° or 25° for the MRS, with continuous coverage of 47° through 55° in the nonfocussing spectrometer.

III. THEORETICAL CALCULATIONS

One advantage of exclusive measurements for studying the NN interaction is that there exist more concise reaction models with which to interpret the data. This is offset in some degree by the greater complexity of dealing with distortions from multiple scattering in two exit channels as well as the incident channel. Distorted wave impulse approximation (DWIA) models for the exclusive knockout reaction have three essential components which can be specified independently. The bound state wave function of the struck nucleon can be calculated in a suitable potential and is strongly constrained by electron scattering data [28,29]. The

representation for the main interaction can be chosen from a set including the free amplitudes calculated from phase shifts [30,31], as well as models for density dependence [19,32]. Finally, the distorting optical potentials are strongly constrained by proton elastic scattering data as well as microscopic theoretical calculations [33]. Spin observables are expected to be less sensitive to the choice of optical potential because they are ratios of cross section combinations, as shown in reference [34]. This is the case especially for knock-out of s-state nucleons, where there is no effective initial polarization of the struck nucleon [20].

Although phenomenological optical potentials have been routinely invoked in the interpretation of many nuclear studies with hadronic probes over the past decades, it is only relatively recently that they have been placed on a firmer foundation of microscopic calculations based on the ''elementary'' nucleon-nucleon interaction [30,31]. The shapes of the real part of the potentials that have emerged in the nonrelativistic framework are dramatically different from nuclear matter density distributions [35]. Such information about the potential near the center of the nucleus, which can be crucial in the interpretation of reaction data, is impossible to derive from elastic scattering measurements alone.

Relativistic optical models based on the Dirac equation have reestablished a more direct link between the shape of nuclear matter distributions and potentials that accurately represent a large body of elastic scattering data [33]. Nuclear reaction calculations based on this Dirac picture offer new hope for quantitative interpretation of data for hadronic probes. The multidimensional kinematic phase space available in $(p,2p)$ experiments allows considerable flexibility in the choice of the kinematic parameters of the final state, even while constraining the energies defining the final state distorted waves [36]. For example, we may use this flexibility to minimize off-shell effects, while we vary the energies and angles of the final state protons to make redundant comparisons of the predictions of DWIA calculations with data. In this way, we may test the validity of scattering wave functions inside the nucleus. In the context of the present experiment with ^{16}O, we might expect that the analyzing powers for p-state knockout, which are typically strongly affected by the struck nucleon effective polarization, will constitute a test of the optical potentials. On the other hand, the $1s$ protons can have no such polarization.

A. Nonrelativistic DWIA

Distorted wave impulse approximation calculations were carried out using the most recent version of the code THREEDEE [37]. This code employs a zero-range nonrelativistic approach in which the bound state and distorted wave functions are two-component spinors. However, it does employ relativistic kinematics. Due to the inclusion of spin-dependent terms in the nucleon-nucleus optical potentials, factorization into a distorted momentum distribution and nucleon-nucleon cross section is not possible. For economy in the calculation, the transition amplitude can still be factorized into products of distorted wave amplitudes and two-body p-p amplitudes evaluated at the asymptotic kinematics. However even this simplification can now be dispensed with in order to include a radial density-dependence in the two-body amplitudes.

Distorted waves were generated using a Schrödinger equivalent reduction of the global Dirac analysis by Cooper *et al.* [38]. The bound state wave functions were computed using a Woods-Saxon potential with parameters taken from a DWIA analysis of ^{16}O$(e,e'p)$ data at NIKHEF [28]. In that work the geometrical parameters of the bound state potential, defining the rms radii of the single particle wave functions, were chosen to reproduce the measured spectral functions.

For density independent calculations (calculations denoted here as STD) the nucleon-nucleon t matrix was evaluated from the free scattering phase shifts at the final state N-N relative momentum. Density dependent modifications to this two-body t matrix were included in a local density approximation with a t matrix computed according to Horowitz and Iqbal [2] (denoted by DD-STD), in which the density dependence is assumed to arise from modifications to the nucleon effective mass due to the large Lorentz scalar potential in the nuclear interior.

Calculations were also carried out using an empirical density dependent nucleon-nucleon interaction, as described by Kelly *et al.* [18] (these calculations are denoted as DD-RAY). The particular choice of the effective interaction presented in this work is that of Ray [32], an interaction which in the limit of zero density gives good fits to the N-N phase shifts up to 1 GeV. Ray used this interaction to fit proton-nucleus elastic scattering data from 320 to 800 MeV, and showed that the density dependence was important even at the highest energies. Due to the fact that this interaction was fitted at a few discrete energies, there are some differences between the two-body observables predicted by the phase shifts and those by the Ray effective interaction for zero density. However, these are primarily for the 25° calculations and the differences are sufficiently small for the N-N analyzing power that they do not alter the conclusions reached in this paper.

B. Relativistic DWIA

A new DWIA calculation in the Dirac framework has been developed [34]. It incorporates Dirac optical potentials globally fitted to elastic scattering data, but guided by relativistic mean field theory. The fundamental interaction is represented as a relativistic Love-Franey t matrix. It is treated in finite range, potentially resulting in more sensitivity to its off-shell properties, which are probed by distortions as well as by the usual kinematic effects. It is expected that the strong explicit dependence on the Mandelstam s appearing in the nonrelativistic representation of the interaction, which is difficult to treat accurately in $(p,2p)$ calculations, is largely included implicitly in the Dirac spinors [39]. Of course, the spinors also directly experience the density dependent lower-component enhancement, a simple model of which is included as one of the options for the nonrelativistic calculations described above.

The application of this calculation to a nucleus as light as ^{16}O has required considerable effort in understanding how to cope with a three-body problem in a Dirac framework. This has now been achieved [40]. The agreement with $(p,2p)$ data is quite good at 200 MeV, although the calculation is sensitive to the choice of optical potential at certain kinematics. At 500 MeV, the impulse approximation should be more

reliable, but recoil effects are larger. Without the recent advances in the treatment of recoil momentum in the Dirac model calculation, comparison of this model with the present data would have been impossible.

IV. RESULTS AND ANALYSIS

Uncertainties in the absolute thickness of the waterfall target precluded the extraction of cross sections in this experiment. Therefore for comparisons with the calculations in this paper, cross section data were taken from another experiment [23] which had very similar kinematic conditions. The analyzing power, on the other hand, is sensitive only to the relative thickness of the target correlated with beam polarization. The flow of water to the target was regulated, so that the target thickness varied only slowly, whereas the beam polarization was cycled on a few-minute interval. Each measurement required several hours, so the average target thickness is assumed to be the same for both beam spin states. The monitor of p-p elastic events from the target showed no significant variation of the target thickness for the different spin states.

The peak fits to the missing mass spectrum, exemplified in Fig. 2, were constrained by the known separation energies of the proton bound-state orbitals from electron scattering results [28]. The observed widths of the ground-state $1p_{1/2}$ and 6.3 MeV $1p_{3/2}$ peaks were due entirely to the experimental resolution. Hence the same widths were used for these peaks as well as for the additional contribution from two $\frac{3}{2}^-$ states at about 10 MeV, due to $2p$-$2h$ excitations in the ground-state wave function [28]. The broad peak from knock-out from the $1s_{1/2}$ orbital was fit with free parameters for its position and width. The fitted spectra were first corrected for background events from accidental coincidences. A linear background due to four-body final states, multiple scattering, etc. was included. This background is relatively small in the kinematic region relevant for s-state knockout, as evidenced by the immediate surrounding region. We estimate that two-step reaction contributions are less than 10% of the area under the s-state peak, and most of this is removed by the background subtraction. This background is least important in comparison with the large cross sections near zero recoil momentum where the data more clearly constrains the two-body interaction, as will later be discussed.

A. Cross sections

As a first step, in Figs. 3 and 4 we compare the standard DWIA calculations (STD) to the ^{16}O$(p,2p)^{15}$N cross section data of Ref. [23]. These data were obtained at an incident energy of 500 MeV with one emitted proton detected at $\theta_1 = 22.15°$ and the second at various angles centered about the quasifree point. In the figures we present the data for six of the published angle pairs ranging from 40.3° to 72.3°. The agreement with the cross section data is rather good, particularly near the quasifree angle. However it tends to deteriorate somewhat at the forward angles, with the DWIA producing a broader distribution than the data. For each state in ^{15}N a single overall spectroscopic factor has been used. The extracted spectroscopic factors are $C^2S = 1.05$ for the $p_{1/2}$ ground state and $C^2S = 2.0$ for the $p_{3/2}$ excited state. These spectroscopic factors are in very good agreement with those

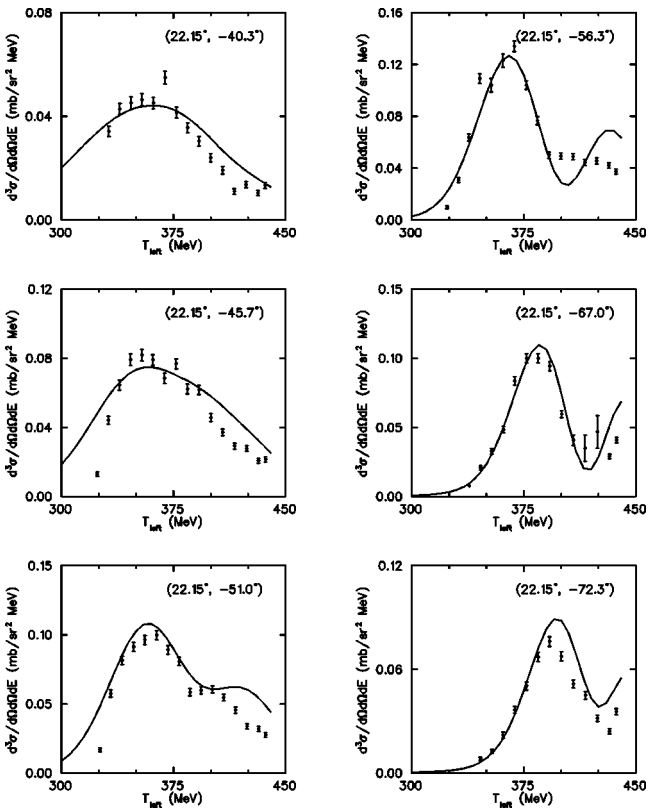

FIG. 3. Energy sharing cross sections for the ^{16}O$(p,2p)^{15}$N ($\frac{1}{2}-$, ground state) reaction at 504 MeV. The curves are standard DWIA calculations (STD) as described in the text, normalized with a spectroscopic factor of $C^2S = 1.05$.

extracted from the analysis of ^{16}O$(e,e'p)$[28]—respectively 1.17 and 2.24—and are well within the errors in the absolute cross sections [about 15% for the $(p,2p)$ data]. We note again that in our analysis we used the same rms radii for the two bound states as in Ref. [28].

Overall the DWIA gives an adequate description of the cross section data. The p-shell knockout cross sections for the other DWIA calculations that include density dependence are very similar to those in the figures, with differences typically less than 10%. It is for the analyzing powers that the density dependence has a large effect.

B. Analyzing powers

The analyzing powers for proton knockout from the $1p_{1/2}$, $1p_{3/2}$, and $1s_{1/2}$ orbitals of ^{16}O are shown in Figs. 5, 6, and 7, respectively. The data are compared with nonrelativistic DWIA calculations using the three different interactions described in the previous section: the STD calculation—standard NN phase shifts with no density dependence [37] (solid); the DD-STD calculation—same as the STD calculation with density dependence added according to the prescription of Horowitz and Iqbal [2] (dashed); and the DD-RAY calculation, an empirical density dependent nucleon-nucleon interaction from Ray, *et al.* [18] (dotted). All calculations use the same optical model potentials and bound-state wave functions as given in Sec. III A above.

In general the STD calculations (solid line) with no density dependence predict an analyzing power larger than the data, particularly for 20°. This is true for all three states, but

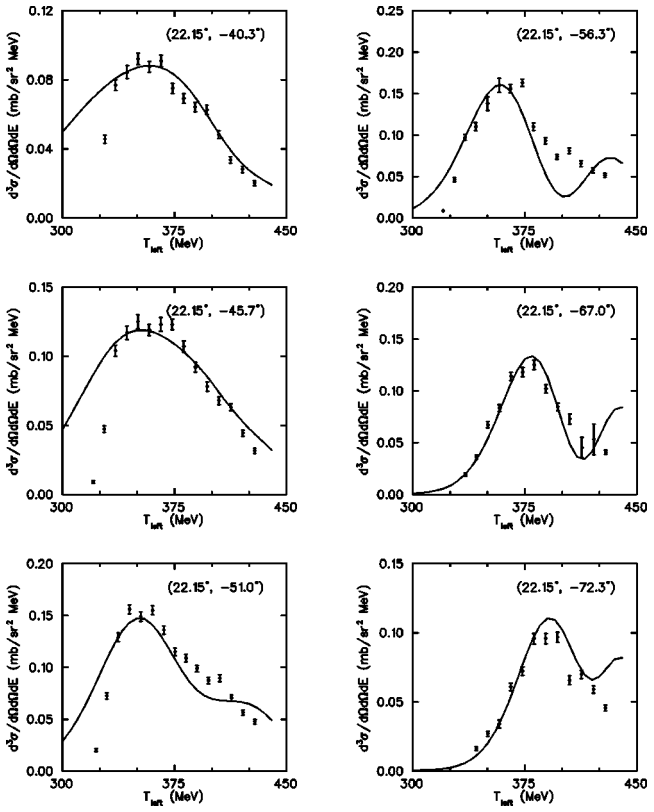

FIG. 4. Energy sharing cross sections for the ^{16}O$(p,2p)^{15}$N ($\frac{3}{2}-$, 6.3 MeV state) reaction at 504 MeV. The curves are standard DWIA calculations (STD) as described in the text, normalized with a spectroscopic factor of $C^2S=2.0$.

the disagreement is especially large for the $1s_{1/2}$ state. As mentioned previously, knockout from the $1s_{1/2}$ state does not involve a distortion-induced bound-state nucleon polarization, and is most affected by medium modifications, since the struck nucleon wave function has its maximum at the center of the nucleus. In the absence of in-medium effects, we would have expected the analyzing power data for the $1s_{1/2}$ knockout to follow the solid curve in Fig. 7. A comparison of $1p_{1/2}$ (Fig. 5) and $1p_{3/2}$ (Fig. 6) knockout reveals substantial differences due to the effective struck nucleon polarization, both in the data and in the STD calculations, and especially at 20°. This polarization, generated by the central terms in the optical potentials, has the opposite sign for $1p_{1/2}$ and $1p_{3/2}$ knockout. All the analyzing power data are poorly reproduced by the STD calculation.

The dashed lines show the DD-STD results of approximating the effects of enhancement of the lower components of the Dirac spinors in a large nuclear scalar potential which lowers the effective mass of the protons [2]. Although this effect is included implicitly in the Dirac-based calculations of Cooper *et al.* [38], it is interesting to try to distinguish this effect from other differences between relativistic and nonrelativistic calculations. The lower component enhancement has the effect of reducing the DD-STD analyzing powers by roughly 15–20 % for the tightly bound $1s_{1/2}$ state. This suppression of the analyzing powers in exclusive $(p,2p)$ is greater than that predicted for inclusive quasifree scattering.

Somewhat surprisingly, the other nonrelativistic calculation (DD-RAY, dotted line), using the density dependent interaction of Ray [32] produces results very similar to those of the DD-STD calculation. The density dependent suppression in the two models would seem to be of different origin, yet the results are very similar. At 25° both calculations provide a relatively good description of the $1p_{1/2}$ and $1p_{3/2}$ knockout data. Also the magnitude of the analyzing power for the higher energy portion of the 25° $1s_{1/2}$ knockout data is nearly correct, but the slope to lower energies is too steep. In contrast, with the exception of the high energy portion of the $1p_{3/2}$ state, the overall analyzing power predictions for 20° are in poor agreement with the data. Although the density dependence in the calculations does provide some suppression of the analyzing powers, this suppression is insufficient. The reason for this disagreement is not understood. Although there are concerns about the particular choice of optical model potential for the low energy emitted proton, we note that good agreement is obtained at 25° which has a comparable range of energies. Furthermore the disagreement is greatest on the left side of the figures where the low energy proton has roughly 120 MeV and the distorted wave treatment should be reasonable. In spite of these problems, the clear trend is that both interaction models for density dependence reduce the analyzing power from the free *NN* value in the direction required by the data. Thus it is reasonable to conclude that these data give evidence for substantial modification of the *NN* interaction in the nuclear interior.

As a final comparison, we reproduce as the dash-dot curve in Figs. 5, 6, and 7 the results obtained with the complete finite-range Dirac-based calculation [41]. The Dirac optical potentials used in these calculations [38] are the global fits from which were derived the two-component reductions used in our nonrelativistic DWIA calculations. As mentioned previously, relativistic medium effects, which are only approximated in nonrelativistic models, are included implicitly in the Dirac-based model. For *p*-shell knockout these calculations show the largest suppression of the analyzing powers, in some cases significantly larger than predicted by the approximate models in the Schrödinger context. For two angles the predicted analyzing powers are even below the data. On the other hand, this calculation is the least successful for the case of $1s$ knockout. The large slope as a function of energy sharing is even more pronounced than with the nonrelativistic calculations. As we show in Sec. IV D, the large extraneous slope predicted for the analyzing power may arise from the spin-orbit part of the optical potential, suggesting a fundamental defect in these optical potentials.

C. Spin transfer

The spin-observables D_{SS} and D_{SL} are shown in Fig. 8 as a function of the low-energy proton angle. The MRS is a vertical-bend spectrometer, and the sideways polarization is not precessed by the magnetic field. However the longitudinal component does precess, requiring a correction factor which depends on the detected focal plane position. Because of the limited statistics due to the secondary scattering required to measure the scattered proton polarization, the data in Fig. 8 have been integrated over the energy-difference

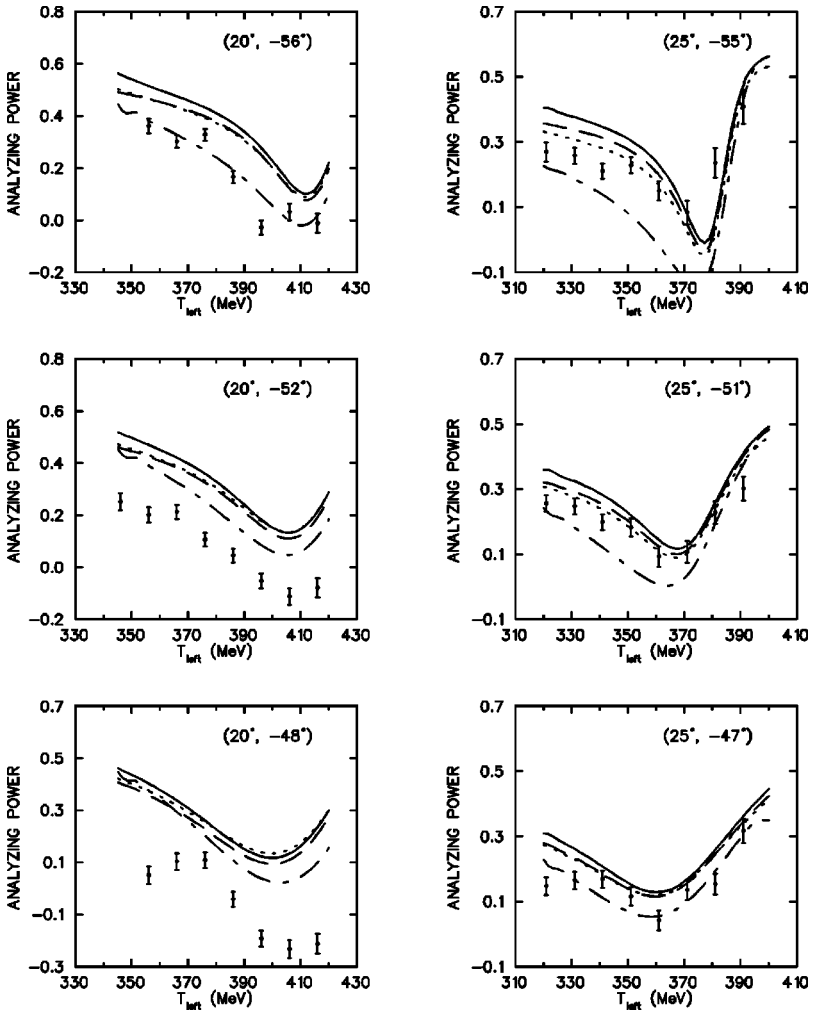

FIG. 5. Analyzing powers for knockout of protons from the $1p_{1/2}$ states in ^{16}O, plotted versus the kinetic energy of forward angle proton. The solid curves (STD) show the calculations using the free p-p interaction, the dashed curves (DD-STD) show the simulated lower component enhancement of Dirac spinors, and the dotted curves (DD-RAY) show the interaction with empirical density dependence. The entirely Dirac-based calculation is shown as the dot-dashed curves.

range corresponding to the 25° angle pairs in the previous figures. The calculations have been averaged over this same range even though there is little variation of D_{SS} and D_{SL} over these energies. No spin observables were extracted for p-shell knockout because of uncertainties associated with fitting the low-statistics $1p_{1/2}$ and $1p_{3/2}$ peaks in the missing mass spectra.

The data in Fig. 8 are the first spin observables ever measured at intermediate energies for the $(p,2p)$ reaction. The data for the D_{SL} variable are smaller than the calculations, although the size of the error bars do not make this conclusive. We note that both the free N-N phase shifts and the Ray interaction at zero density are in excellent agreement with the measured N-N spin-transfer observables. It is interesting that the density-dependence moves D_{SL} slightly more negative, away from the data, whereas for A_y it moves the calculations closer to the data. The D_{SS} data have smaller errors and are significantly larger than any of the calculations. The disagreement between the D_{SS} data and the free-space polarization transfer observable is no surprise, as this situation is also reflected in the inclusive data [8,9]. It does not appear that the present models for density dependence of the interaction are relevant to the discrepancy. Nonetheless, the addition of the polarization transfer data provides a valuable constraint for future theoretical models.

D. Spin orbit effects

One element of the calculation that could strongly affect analyzing powers, even for s-state knockout, is the spin-orbit term in the optical potentials. (The central terms affect $1s_{1/2}$ analyzing powers only weakly, and not at all in DWIA calculations that treat a density-independent interaction in zero-range.) To obtain an indication of how large this effect could be, two sets of calculations were done using the Ray density dependent interaction (DD-RAY), one with the spin-orbit potentials set equal to zero for the incident proton, and the other with them set to zero for both the incoming and emitted protons. The analyzing powers for these calculations are compared to the results of calculations with normal spin-orbit terms in Fig. 9, where the knockout from the $1p_{1/2}$, $1p_{3/2}$, and $1s_{1/2}$ orbitals are shown (top to bottom, respectively) for two angle pairs. The curves are described in the figure caption. The prominent slope as a function of the kinetic energy $T_{\rm left}$ for the $1s_{1/2}$ orbital is nearly eliminated when the spin-orbit potential is set to zero, leaving the ana-

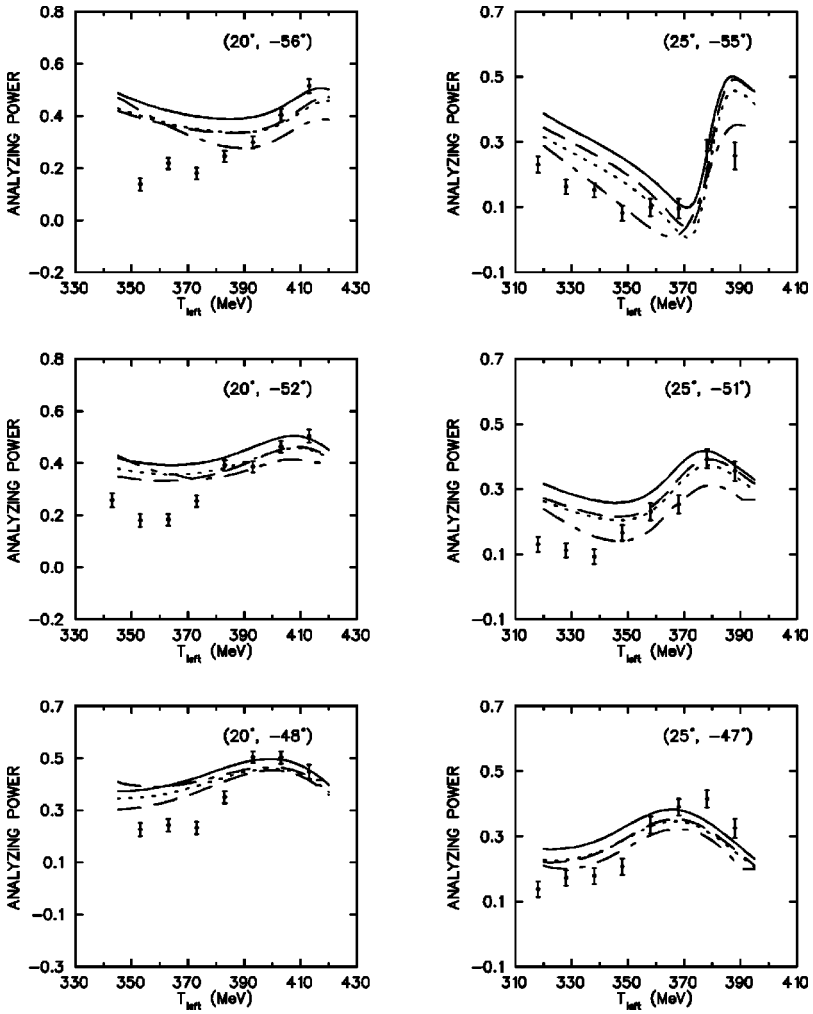

FIG. 6. Analyzing powers for knockout of protons from the $1p_{3/2}$ states in ^{16}O, plotted versus the kinetic energy of forward angle proton. The curves are explained in Fig. 5.

lyzing powers at essentially the values they had near zero recoil momentum (maximum cross section). This tends to improve agreement with the $1s_{1/2}$ data, but has a very negative effect on the calculations for the p-shell knockout, in this case worsening agreement with the data. Of course, distortions cannot legitimately be left out of the calculations. However, this exercise demonstrates the importance of the spin-orbit force in this reaction, and points to the source of the strong slope in the $1s_{1/2}$ calculations. This effect is far beyond what one might have expected. The much larger slope for the fully relativistic calculation presumably is evidence of intrinsic differences between Schrödinger and Dirac calculations, since the interactions and potentials used are nearly equivalent. The results emphasize the necessity for having a good treatment of the optical model potentials throughout the nuclear volume.

The second lesson to be learned from Fig. 9 is that the DWIA $1s_{1/2}$ analyzing powers near the kinematic points of minimum recoil momentum, indicated by arrows in the figures, are insensitive to spin orbit distortions.[1] This can be seen at both angle combinations. Similar behavior has been confirmed with the other interactions used in this paper, and even with a very different set of optical potentials [42]. (There is some indication that the points of minimum sensitivity are more closely related to the maxima in the cross sections, which can vary slightly with the central terms in the optical potentials.) Also, Fig. 7 indicates that even the Dirac prediction is fairly consistent with the others at these points. This insensitivity of the DWIA analyzing powers to the optical potentials has the important implication that these kinematic points provide an opportunity to test two-body interactions *without ambiguities associated with the optical potentials*. Since all the calculations seriously disagree with the data at these points, we are led to the conclusion that all the interactions tested here are seriously deficient, at least in the context of the DWIA.

V. CONCLUSIONS

A measurement of exclusive proton knockout was undertaken in order to learn about the nature of strong interactions at nuclear matter densities. The nucleons bound in the $1s_{1/2}$ orbital in the ^{16}O nucleus are at a high matter density, and are not subject to the effective polarization inherent in

[1]This feature of $s_{1/2}$ knockout did not appear in earlier calculations because of errors in the code that have since been corrected.

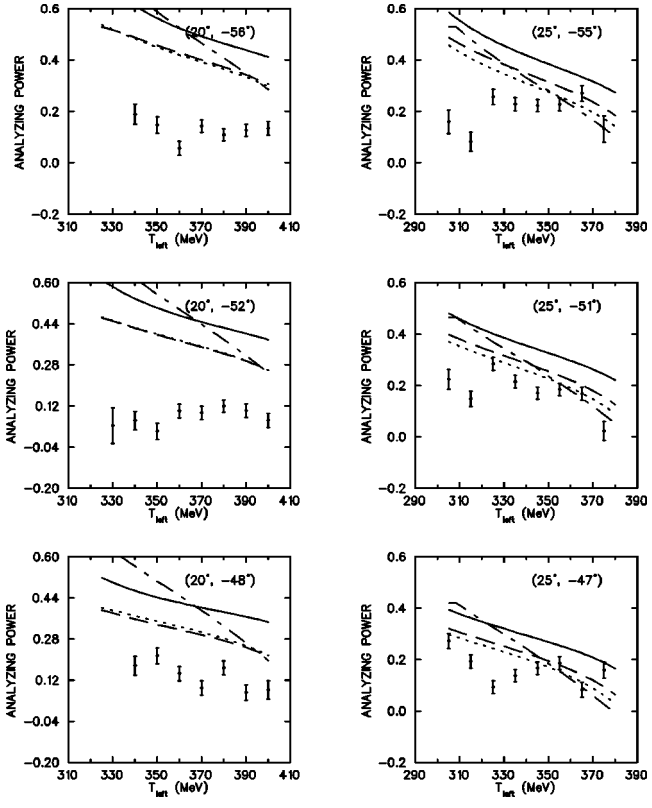

FIG. 7. Analyzing powers for knockout of protons from the $1s_{1/2}$ state in ^{16}O, plotted versus the kinetic energy of forward angle proton. The curves are explained in Fig. 5.

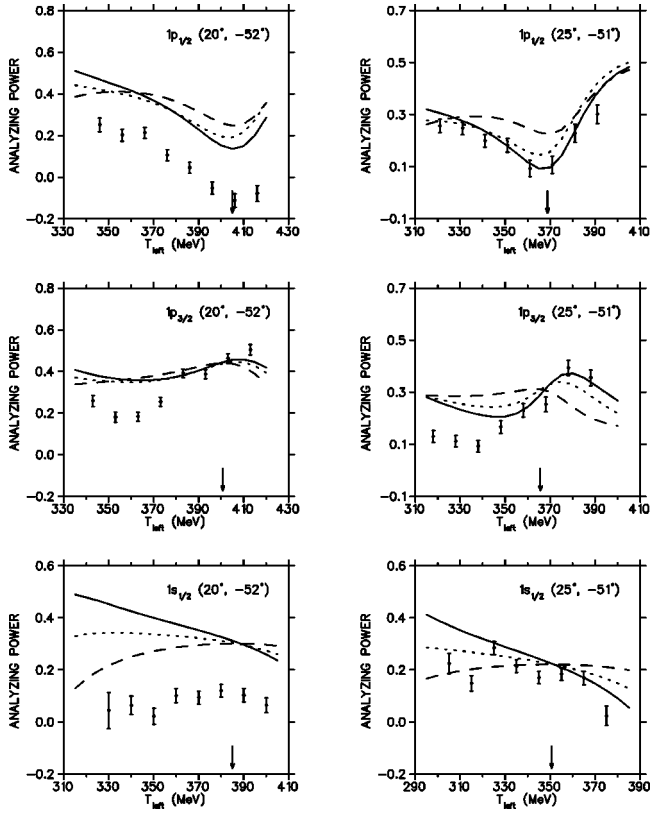

FIG. 9. Analyzing powers for knockout of protons from the $1p_{1/2}$ orbital (top two panels), $1p_{3/2}$ orbital (middle two panels), and $1s_{1/2}$ orbital (bottom two panels) in ^{16}O. The angle pairs are shown in each figure. The analyzing powers are plotted versus the kinetic energy of forward angle proton. The solid curves are the DWIA calculations with the density dependent interaction of Ray (DD-RAY), as presented in Figs. 5–8. The other two sets of curves are the same calculation, but with the spin-orbit potential of the incident proton set to zero (dashed curve) and the spin-orbit potential of both the incident and emitted protons set to zero (dotted curve). The arrows indicate the positions of minimum recoil momentum.

p-state knockout. We have selected kinematics to minimize the nuclear recoil momentum for s-shell knockout, while maximizing the sensitivity of the polarization asymmetry to medium effects.

The $(\vec{p},2p)$ data have been compared to the best available DWIA reaction models. A zero-range Schrödinger based model allows explicit density dependence of the two-body interaction, while a Dirac based calculation employing Lorentz invariant amplitudes fit to the free phase shifts is done in full finite range. Both Schrödinger and Dirac models employed similar bound-state wave functions from $(e,e'p)$ data, and equivalent global optical potentials. Several different two-body interactions were tried in the Schrödinger calculations, including the free interation, one attempting to simulate a medium effect implicit in the Dirac model, and an empirical effective interaction fit to proton-nucleus elastic and inelastic data.

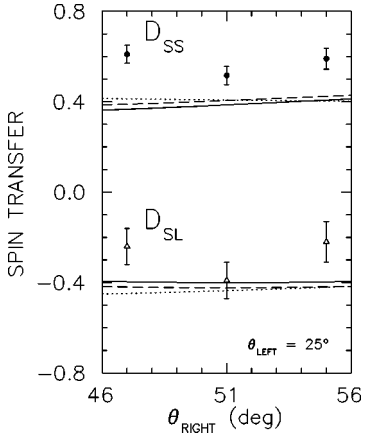

FIG. 8. Spin transfer observables for the knockout of protons from the $1s_{1/2}$ orbital in ^{16}O, for $\hat{s}$-polarized beam. The data are plotted as a function of the low-energy proton laboratory angle. The angle of the high-energy proton was fixed at 25° in the lab. The data and calculations have been averaged over all measured kinetic energies. The curves are explained in Fig. 5.

None of the theoretical models is in good agreement with the data. Although the calculations follow the trend of the data, the measured asymmetries for the $1s$ knockout are typically much smaller than the calculations. Models with density dependence do better, but still are inadequate. The finite range relativistic model does not do much better than its nonrelativistic density-dependent counterpart. The problem is not likely to be in the bound-state wave function, which produces good agreement with ^{16}O$(e,e'p)$ data.

In conclusion, the $(\vec{p},2p)$ data for $1s$-shell knockout exhibit a dramatically reduced analyzing power compared to the free NN value, strengthening the evidence for significant medium modifications to the NN interaction at high densi-

ties. However, the anomalous steep slope of the predicted analyzing powers as a function of the energy sharing between final state protons seems to be associated with spin-orbit distortions, suggesting that the spin-orbit part of the optical potential needs improvement. The $1s_{1/2}$ analyzing powers are very sensitive to the spin-orbit part of the optical potential, except for local insensitivity near the kinematic points of minimum recoil momentum. Hence the persistence of the disagreement between theory and data at these points indicates that the failure of the models cannot be ascribed only to deficiencies in the optical potentials. This enables us to come to a conclusion about the two-body interaction in spite of the fact that all the calculations use the same seemingly imperfect optical model potentials. None of the calculations can adequately describe the analyzing power data, even near zero recoil kinematics, and especially for the $1s_{1/2}$ state, although the models with density dependence come closer to predicting the data than do models without. Hence the data offer equivocal support both for free interactions modified only by distortion of nucleon Dirac spinors in nuclear matter, and for an empirical density-dependent interaction that is widely successful for elastic and inelastic scattering of protons on nuclei. However, it is clear neither are adequate for nucleon knockout. There is scope for further work toward inclusion of more interesting mechanisms for density dependence, such as that mentioned in connection with Refs. [15–17]

The D_{SL} polarization transfer observable is in agreement with the predictions based on the free-space N-N interaction, whereas the data for D_{SS}, which have better statistical precision, are not well described by any of the models. These data are expected to provide another constraint on future models of the density-dependent N-N effective interaction.

ACKNOWLEDGMENTS

We would like to thank the support of NSERC and the NSF for funds to complete this project. We especially thank Oren Maxwell and Tim Cooper for helpful discussions, and for kindly providing the Dirac model calculations.

[1] Y. Mardor *et al.*, Phys. Rev. Lett. **65**, 2110 (1990), and references therein.
[2] C. J. Horowitz and D. P. Murdock, Phys. Rev. C **37**, 2032 (1988); C. J. Horowitz and M. J. Iqbal, *ibid.* **33**, 2059 (1985).
[3] C. Mahaux and R. Sartor, in *Advances in Nuclear Physics*, edited by J. W. Negele and E. Vogt (Plenum, New York, 1990), Vol. 20.
[4] G. E. Brown, C. B. Dover, P. B. Siegel, and W. Weise, Phys. Rev. Lett. **26**, 2723 (1988).
[5] N. M. Hintz *et al.*, Phys. Rev. C **30**, 1976 (1984).
[6] T. A. Carey *et al.*, Phys. Rev. Lett. **53,** 144 (1984).
[7] C. Glashausser, *et al.*, Phys. Rev. Lett. **58**, 2404 (1987).
[8] C. Chan *et al.*, Nucl. Phys. **A510**, 713 (1990).
[9] O. Häusser *et al.*, Phys. Rev. C **43**, 230 (1991).
[10] K. H. Hicks, in *Intersections Between Particle and Nuclear Physics*, Proceedings of a Conference held in Rockport, ME, 1988, edited by Gerry M. Bunce, AIP Conf. Proc. No. 176, (AIP, New York, 1988), p. 26.
[11] R. D. Smith and J. Wambach, Phys. Rev. C **36**, 2704 (1987); H. Esbensen and G. F. Bertsch, *ibid.* **34**, 1419 (1985).
[12] R. J. Furnstahl and S. J. Wallace, Phys. Rev. C **47**, 2812 (1993).
[13] N. Ottenstein, S. J. Wallace, and J. A. Tjon, Phys. Rev. C **38**, 2272 (1988).
[14] E. Rost and J. R. Shepard, Phys. Rev. C **35**, 681 (1987).
[15] G. E. Brown, M. Buballa, Zi Bang Li, and J. Wambach, Nucl. Phys. **A593**, 295 (1995).
[16] E. J. Stephenson, J. Liu, A. D. Bacher, S. M. Boyer, C. Chang, C. Olmer, S. P. Wells, S. W. Wissink, and J. Lisantti, Phys. Rev. Lett. **78**, 1636 (1997).
[17] N. M. Hintz, A. M. Lallena, and A. Sethi, Phys. Rev. C **45**, 1098 (1992).
[18] H. Seifert *et al.*, Phys. Rev. C **47**, 1615 (1993), and references therein.
[19] J. J. Kelly and S. J. Wallace, Phys. Rev. C **49**, 1315 (1994).
[20] P. Kitching *et al.*, Adv. Nucl. Phys. **15**, 43 (1985).
[21] C. A. Miller *et al.*, in *Proceedings of the 7th International Conference on Polarization Phenomena in Nuclear Physics, Paris, 1990* (Editions de Physique, Les Ulis, France, 1990), p. C6-595.
[22] K. Hatanaka *et al.*, Phys. Rev. Lett. **78**, 1014 (1997).
[23] W. J. MacDonald *et al.*, Nucl. Phys. **A456**, 577 (1986).
[24] R. Abegg and R. Schubank, TRIUMF Design Note TRI-DN-87-17, 1987 (unpublished).
[25] B. Larson *et al.*, Phys. Rev. C **53**, 1774 (1996).
[26] C. A. Miller, TRIUMF Report TRI-83-3, p. 339, 1983 (unpublished).
[27] O. Häusser *et al.*, Nucl. Instrum. Methods Phys. Res. A **254**, 67 (1987); R. S. Henderson *et al.*, *ibid.*, **254**, 61 (1987).
[28] M. Leuschner *et al.*, Phys. Rev. C **49**, 955 (1994).
[29] S. Frullani and J. Mougey, Adv. Nucl. Phys. **14**, 1 (1984).
[30] M. A. Franey and W. G. Love, Phys. Rev. C **31**, 488 (1985).
[31] J. A. McNeil, J. R. Shepard, and S. J. Wallace, Phys. Rev. Lett. **50**, 1439 (1983).
[32] L. Ray, Phys. Rev. C **41**, 2816 (1990).
[33] B. C. Clark, S. Hamma, S. R. Mercer, L. Ray, and B. Serot, Phys. Rev. Lett. **50**, 1644 (1983); C. J. Horowitz and D. Murdock, Phys. Rev. C **35**, 1442 (1987).
[34] E. D. Cooper and O. V. Maxwell, Nucl. Phys. **A493**, 468 (1989); **A513**, 584 (1990).
[35] H. O. Meyer *et al.*, Phys. Rev. C **37**, 544 (1988); K. H. Hicks *et al.*, *ibid.* **38**, 229 (1988).
[36] A. A. Ioannides and D. F. Jackson, Nucl. Phys. **A308**, 305 (1978).
[37] N. S. Chant and P. G. Roos, Phys. Rev. C **27**, 1060 (1983).
[38] E. D. Cooper *et al.*, Phys. Rev. C **47**, 297 (1993); S. Hama, B. C. Clark, E. D. Cooper, H. S. Sherif, and R. L. Mercer, *ibid.* **41**, 2737 (1990).
[39] E. D. Cooper (private communication).
[40] O. V. Maxwell and E. D. Cooper, Nucl. Phys. **A565**, 740 (1993).
[41] O. V. Maxwell and E. D. Cooper, Nucl. Phys. **A574**, 819 (1994).
[42] A. Nadasen *et al.*, Phys. Rev. C **23**, 1023 (1981).